

Permeation of n-butane, 1-butene and 1,3-butadiene through anhydrated Ag⁺-doped perfluorocarbon-type ion-exchange membranes

Kunihiro Adachi^a, Wei Hlu^a, H. Matsumoto^a, Kenji Ito^b and Akihiko Tanioka^{a,*}

^aDepartment of Organic and Polymeric Materials, Tokyo Institute of Technology, 2-12-1, Ookayama, Meguro-ku, Tokyo 152, Japan

^bResearch Center for Advanced Science and Technology, The University of Tokyo, 4-6-1, Komaba, Meguro-ku, Tokyo 153, Japan

(Received 2 May 1997; revised 9 June 1997)

The characterization of anhydrated Ag⁺-doped polyperfluorosulfonate membrane (PSM) was made by using EDS, positron annihilation lifetime measurement and AFM. It was confirmed that the distribution of doped Ag⁺ in the membrane was homogeneous, the membranes were rather dense ones and the concentration of doped Ag⁺ was about twice as much as that of charged group SO₃⁻ in the membrane. The permeation experiments were also carried out for n-butane, 1-butene and 1,3-butadiene. Anhydrated Ag⁺-doped PSM exhibited relatively high permeability for 1-butene compared with n-butane and 1,3-butadiene. The ideal separation factor of 1-butene/n-butane, which was the permeability coefficient ratio of 1-butene to n-butane, was about 5400 in the membranes exchanged by AgNO₃ aqueous solution at 25°C. Both the permeability of 1-butene and selectivity of 1-butene/n-butane increased with decrease of temperature. On the other hand for 1-butene/1,3-butadiene system, the highest ideal separation factor 11.7 was obtained at 70°C while permeability increased with decrease of temperature. The permeation behaviour of alkenes through anhydrated Ag⁺-doped PSM could be explained by a swelling model suggested in this paper. Based on such swelling mechanism, the diffusivity and permeability of alkenes were strongly affected by the amount of alkenes absorbed in the membrane. © 1998 Published by Elsevier Science Ltd. All rights reserved.

(Keywords: Ag⁺-doped polyperfluorosulfonate membrane; paraffin; olefin)

INTRODUCTION

Polyperfluorosulfonate membranes (PSM) have been widely used in industrial separation processes like chlor-alkali cells^{1,2}, fuel cells^{3–5} and selective electrodes^{6,7}. PSM in Ag⁺ form showed high permselectivity in the separation of alkenes from their corresponding saturated compounds and also in the separation of alkenes of different kinds^{8–13}. These phenomena were always considered due to the facilitated transport of alkenes by Ag⁺ in the membrane. The research on the affinity between silver ion and alkene can be dated back to 1938, when Winstein and his co-workers published their first paper about alkene–silver coordination complex¹⁴. Now it is commonly understood that the interaction between the alkene and the silver ion can be described in the following way as shown in *Figure 1*: a σ -type bond, as a result of donation of π -electrons from the occupied 2p bonding orbital of the olefinic system into the vacant 5s orbital of the silver ion, and a π -type bond, as a result of back-donation of d-electrons from occupied 4d orbitals of the silver ion into the unoccupied $\pi^* - 2p$ antibonding orbitals of the olefinic system^{14,15}.

Based on this special interaction, facilitated transport with silver ions as a carrier in various kinds of membranes such as supported liquid membranes and hydrated ion-exchange membranes has been investigated^{16–19}. Gierke performed the research work on hydrated PSM and derived a cluster-network model which suggested that the polymeric

ions and absorbed water separated from the fluorocarbon matrix into approximately spherical domains (with diameter of about 4 nm) connected by short narrow channels of 1 nm width. The average distance between these ion-clusters was about 5 nm. Gases followed this kind of path when they transported through the membrane^{20–22}. Even though these facilitated transport membranes containing Ag⁺ can offer high selectivity for olefin/paraffin separations, supported liquid membranes often have stability problems because of solution loss, while for hydrated Ag⁺-exchanged PSM, we usually have to face the problem of maintaining humidity during operation.

Noble derived a theory to explain facilitated transport of neutral molecules across fixed site carrier membranes²³. The model reduced to a form analogous to dual-mode transport in the reaction equilibrium (diffusion-limited). Based on this model, the transport of gases through fixed site carrier membranes could be described in two parallel ways. One was the simple solute diffusion and the other was the solute hopping between fixed sites. Rabago *et al.* did further research on the facilitated transport fluxes for feed solutions containing 1,5-hexadiene, 1-hexene and n-hexane in hydrated Ag⁺-PSM²⁴. The data and analysis presented in his paper also showed that two transport pathways operated in parallel. One pathway was diffusion in nature and responded to changes in membrane thickness and solute concentration in the expected ways. The other pathway resulted in membrane fluxes that were thickness-independent and possibly independent of the solute concentration in the membrane. The two pathways exhibited different

* To whom correspondence should be addressed

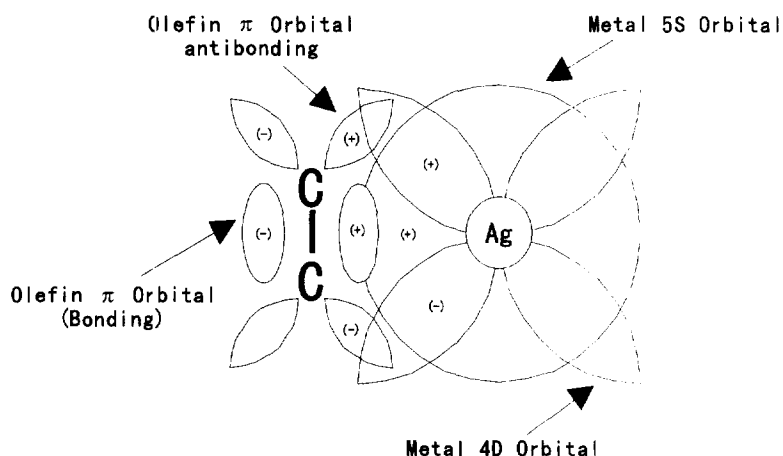


Figure 1 Metal-olefin coordination

selectivity for dienes *versus* monoenes resulting in separation factors for these compounds which were dependent on membrane thickness. However, the physical property of the two transport pathways was not clearly demonstrated.

In this work, the structure of Ag⁺-doped PSM was investigated by using electron microprobe X-ray microanalysis (Energy Disperse X-ray Spectrometer: EDS), positron annihilation lifetime measurement and atomic force microscope (AFM). Then the permeation behaviour of *n*-butane, 1-butene and 1,3-butadiene through anhydrous Ag⁺-doped PSM was studied. Understanding the transport mechanism of alkenes through anhydrous Ag⁺-doped PSM was the objective of this paper.

EXPERIMENT

Membrane preparation

PSM with Na⁺ as counter ions were obtained from Asahi Chemicals. The membranes were immersed in AgNO₃ (Wako Chem.) or AgBF₄ (Aldrich) aqueous solutions for more than 24 h to convert them to the silver form ion-exchange membranes. The concentration of Ag⁺ solution was 1N, 2N and 5N, respectively, and the membrane thickness was 15, 30 and 60 μm, respectively. Then the membranes were taken out from the solution. After the solution on the surface of the membranes was wiped off carefully, the membranes were vacuum-dried at 70°C for more than 12 h. The membranes were kept in a desiccator after drying.

The treatments cited above were performed in a dark chamber because AgNO₃ and AgBF₄ were photosensitive. The reason why AgBF₄ was chosen as the silver salt in this study is that anhydrous silver nitrate can form an explosive complex with 1,3-butadiene²⁵.

Equivalent weight and thicknesses of membranes are listed in Table 1.

Table 1 Properties of perfluorotype ion exchange membrane

Charged group	EW (g mol ⁻¹)	Counter ion	Thickness (μm)
-SO ₃ ⁻	950	Ag ⁺	60
			30
			15
		Na ⁺	30

EW: equivalent weight = membrane weight (dry)/equivalent of charged group

Membrane characterisation

Energy dispersive X-ray spectrometer (EDS). The cross-section of anhydrous Ag⁺-doped PSM were observed by EDS image at 25°C, and together with the EDS line analysis along the direction of membrane thickness, the distribution of Ag⁺ inside the membranes was monitored. EDS area analysis was also carried out to give the information about the quantity of silver ion doped into the membranes.

Positron annihilation lifetime measurement. The size of free volume voids inside the membranes was investigated by positron annihilation lifetime measurement. The positron annihilation lifetime measurement also pointed out the temperature dependence of free volume in the Ag⁺-doped membranes.

Atomic force microscope (AFM). The surface of PSM were observed by atomic force microscope in order to find pores on the membranes.

Permeation measurement. The permeation experiments were carried on the gas permeation apparatus as shown in Figure 2 at different temperatures and feed side pressures for *n*-butane, 1-butene and 1,3-butadiene, respectively. Feed gas from a gas tank was supplied to the high pressure side of the permeation cell through a gas regulator and the pressure was monitored by a pressure sensor (MKS Baratron 390HA-01000SP05). Permeated gas across the membrane was detected by a pressure sensor (MKS Baratron 122AA-01000BB) and the pressure change was recorded as a function of time. Then the pressure was converted to the amount of gas [cm³(STP)]. After non steady-state, the steady-state is established and the relationship between the amount of gases which penetrate through the membrane and the time becomes a straight line. The permeability coefficient *P* can be calculated from the slope of the straight line with equation (1).

$$P = \frac{dP}{dt} \frac{V \cdot 273}{760 \cdot T} \frac{1}{A} \frac{1}{p_1} \quad (1)$$

and the diffusion coefficient *D* can also be obtained from the intercept of the straight line with time axis *θ* (tag time) by equation (2).

$$D = \frac{l^2}{6\theta} \quad (2)$$

where *l* is the thickness of the membrane.

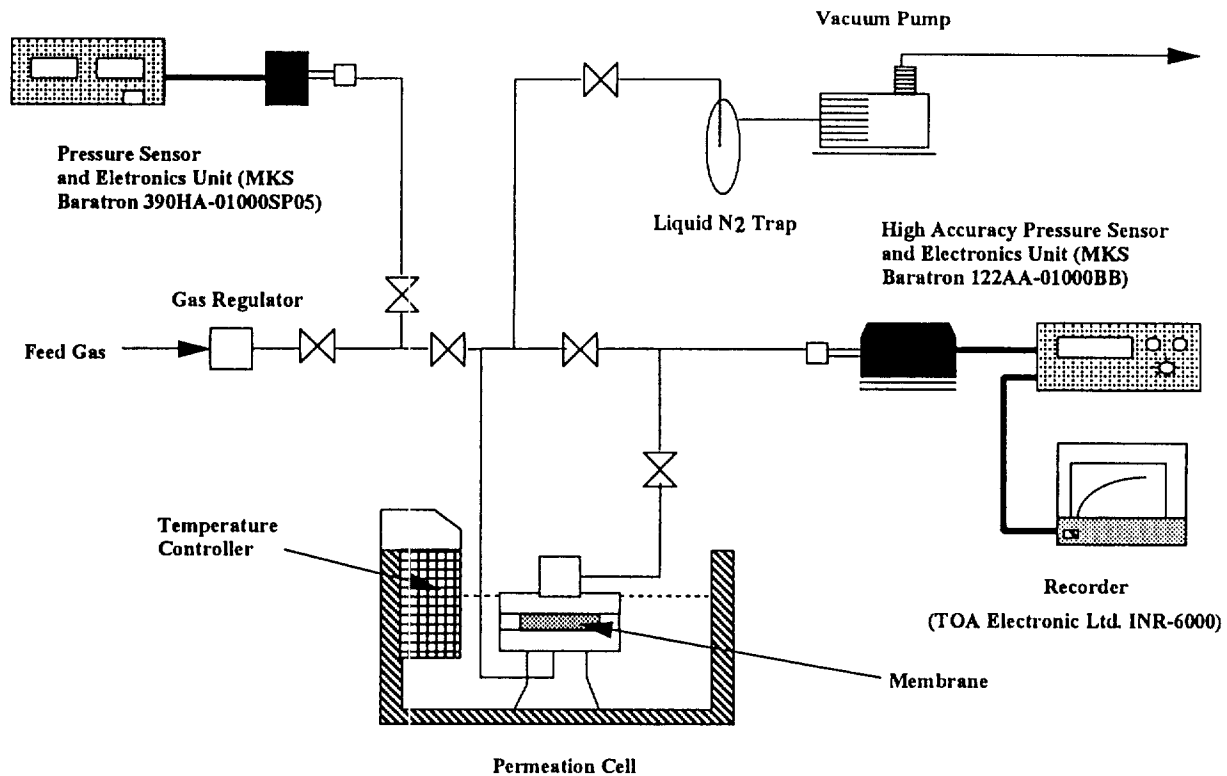


Figure 2 Schematic diagram of gas permeation apparatus

RESULTS AND DISCUSSION

Distribution of silver ion in Ag^+ -doped PSM

Figure 3 shows an EDS image of the cross-section of PSM ($30\ \mu\text{m}$) doped with 2N AgNO_3 and Figure 4 gives the result of EDS line analysis of Ag^+ concentration along the thickness direction of PSM ($60\ \mu\text{m}$) doped with 2N AgNO_3 as indicated by an arrow. The results of PSM doped with other concentrations of Ag^+ solution or PSM of other thicknesses are all the same. This testifies that Ag^+ ions are distributed homogeneously along the direction of membrane thickness. No inhomogeneous aggregation of silver ions on the surface of the membranes is observed regardless of the Ag^+ solution being AgNO_3 or AgBF_4 .

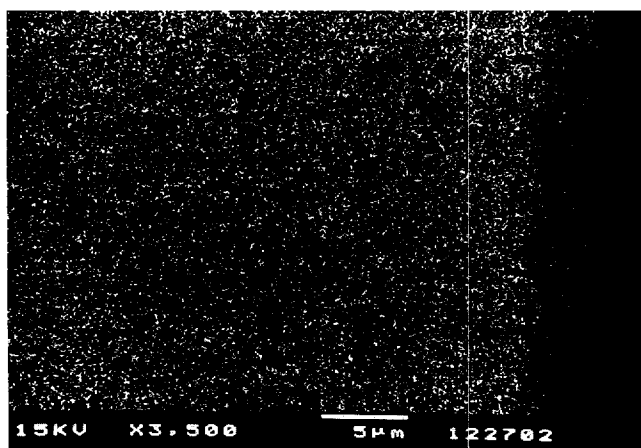


Figure 3 Distribution of Ag in PSM ($30\ \mu\text{m}$) doped with 2N AgNO_3 by EDS image

Concentration of silver ion in Ag^+ -doped PSM

The results of EDS area analysis for S and Ag in Ag^+ -doped PSM are shown in Table 2. The amount of Ag^+ doped in the membrane is about twice as much as that of charged group SO_3^- . This over-dope of Ag^+ means that some of NO_3^- or BF_4^- anions are doped together with Ag^+ into the membrane during the immersing period. Since the separation ability of the membrane is based on the affinity of gas with Ag^+ , this over-doped Ag^+ will improve permeability and selectivity of the membrane for olefin.

Free volume in Ag^+ -doped PSM

Figure 5 shows the AFM image of Ag^+ -doped PSM surface. The existence of the pores whose size are about several hundred Å is not detected.

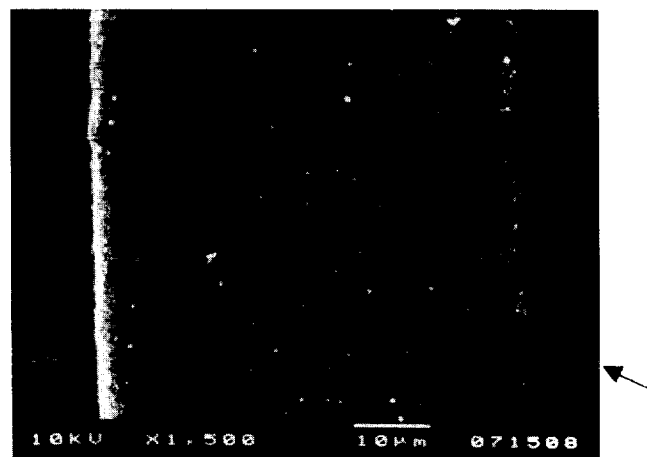


Figure 4 Result of EDS line analysis of Ag for PSM ($60\ \mu\text{m}$) doped with 2N AgNO_3 as indicated by arrow (\leftarrow)

Table 2 Results of EDS square analysis for S, Ag, Na in different types of membrane

Sample (concentration of dopant, thickness)	S (%)	Ag (%)	Na (%)	Sum (%)
Na type (default, 30 μm)	66	—	34	100
Ag type (2N AgNO ₃ , 15 μm)	34	66	—	100
Ag type (2N AgNO ₃ , 30 μm)	33	67	—	100
Ag type (5N AgNO ₃ , 30 μm)	32	68	—	100
Ag type (2N AgBF ₄ , 30 μm)	36	64	—	100
Ag type (5N AgBF ₄ , 30 μm)	27	73	—	100

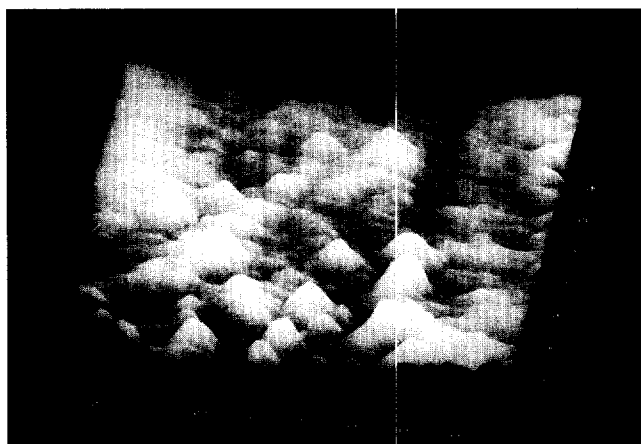
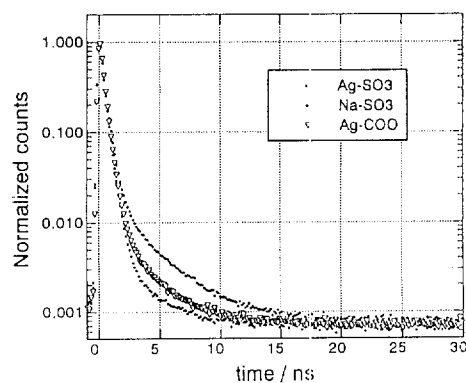

Figure 5 AFM image of PSM surface

Figure 6 Decay curves of positron in different types of membrane

Table 3 Results of positron annihilation lifetime measurement

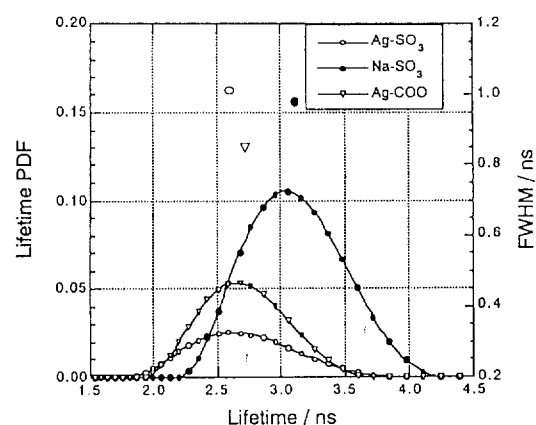
Sample	τ_3	Standard deviation	I_3 (%)	Standard deviation
Ag-SO ₃	2.63	± 0.03	2.8	± 0.0
Na-SO ₃	3.11	± 0.02	10.8	± 0.1

 τ_3 : lifetime of o-Ps

 I_3 : relative intensity of o-Ps

Decay curves of positron lifetime in different types of membranes are shown in *Figure 6* and the analysis results using computer program PATFIT88 and CONTIN are summarised in *Table 3*. *Figure 7* also shows the distribution of lifetime of o-Ps (ortho-positronium) through Laplace transform. The lifetime τ_3 of o-Ps is related to the size of free volume according to the equation:

$$\lambda = 1/\tau_3 = 2\{1 - R/R_0 + \sin(2\pi R/R_0)/2\pi\} \quad (3)$$


Figure 7 Distribution of lifetime of o-Ps in different types of membranes

where R_0 is the radius of free volume, R is the radius of free volume concerning the shielding effect of electrons and the intensity is related to the volume concentration of free volume in the membranes respectively. For each membrane, τ_3 is in the range of 2–5 ns and the free volume size is about several Å which is the same order as in glassy polymer. The anhydrated Ag⁺-doped PSM used in our research are rather dense ones and the travelling paths for gases like cluster network suggested by Gierke do not exist.

The positron annihilation lifetime measurement data for Ag⁺-doped PCM (perfluorocarboxylate membrane) was also given in *Figure 6* and *Figure 7*. However, the discussion about Ag⁺-doped PCM was similar to that of PSM.

Temperature dependence of free volume

Figure 8 shows the temperature dependence of size and number of free volume in Ag⁺-doped PSM. The size of free volume increases with the increase of the temperature and discrete changes happen in two temperature intervals, that is 45–50°C and 65–70°C. This phenomena indicates that there is some kind of membrane structure change in this temperature range.

Permeability of *n*-butane

In *Figure 9* permeability coefficients of *n*-butane through Ag⁺-doped PSM are plotted as a function of reciprocal absolute temperature $1/T$. The permeability coefficient P decreases exponentially with the increase of $1/T$, which is the same tendency as found in the permeation of O₂ in Ag⁺-exchanged PSM²⁶ or *n*-butane in default Na type PSM. The data fell into a rather good straight line according to the active-diffusion theory ($R = 0.9905$). Since the anhydrated Ag⁺-doped PSM used in this research are dense membranes as indicated in the membrane characterization part of this paper, the exhibition of simple solution-diffusion behaviour

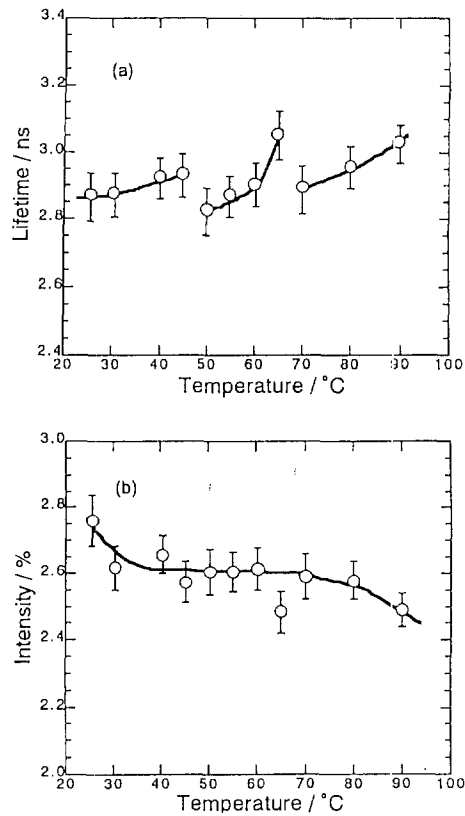


Figure 8 Lifetime (a) and intensity (b) of o-Ps in Ag type PSM as a function of temperature

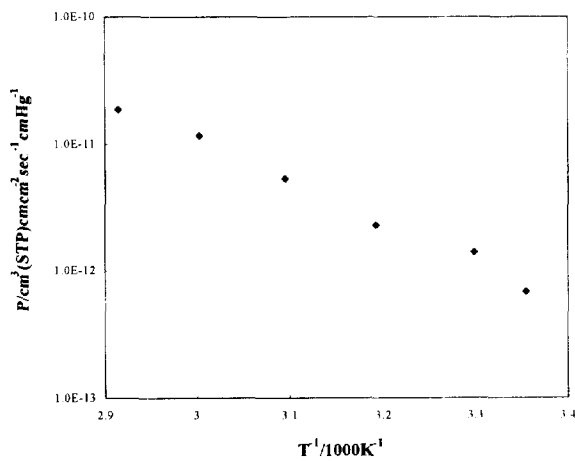


Figure 9 Permeability coefficients of n-butane as a function of reciprocal temperature through PSM doped with 2N AgNO₃ aqueous solution

of n-butane penetrating through the membrane can be clearly understood.

The permeability coefficients of n-butane and O₂ through Ag⁺-doped PSM at 25°C are 6.85×10^{-13} cm³ (STP)-cm/cm²-sec-cmHg and 8.08×10^{-11} cm³ (STP)-cm/cm²-sec-cmHg²⁷, respectively as shown in Table 4. Such difference is mainly attributed to the molecular size which is much larger for n-butane (6 Å) than for O₂ (3.46 Å), therefore the relatively higher resistance should be overcome if n-butane penetrates through the membrane. Table 4 also shows that the permeability coefficient of n-butane in Ag type membrane is smaller than in default Na type membrane. This phenomena can be explained by the fact that the free volume in Ag⁺-doped PSM is smaller than in default Na type membranes.

Table 4 Permeability coefficients of different membrane types and gases

Membrane type	Gas	T (°C)	P (cm ³ (STP)-cm/cm ² -sec-cmHg)
Na	n-butane	25	1.06×10^{-12}
	1-butene	25	1.21×10^{-12}
Ag	oxygen	25	8.08×10^{-11}
	n-butane	25	6.85×10^{-13}
	1-butene	25	3.73×10^{-9}

Permeation of 1-butene

Even though the free volume in Ag⁺-doped PSM is smaller than in Na type membranes, 1-butene exhibits higher permeability than n-butane in Ag⁺-doped PSM as shown in Table 4. Besides this, Figure 10 shows the temperature dependence of permeability coefficient P and Figure 11 shows the temperature dependence of diffusion coefficient D of 1-butene in Ag⁺-doped PSM, respectively. Being opposite to n-butane discussed above, P of 1-butene increases with the reciprocal temperature, while for D, it decreases with temperature below 50°C and then begins to increase as the temperature increases. Such behaviours can not be explained by the simple solution-diffusion model.

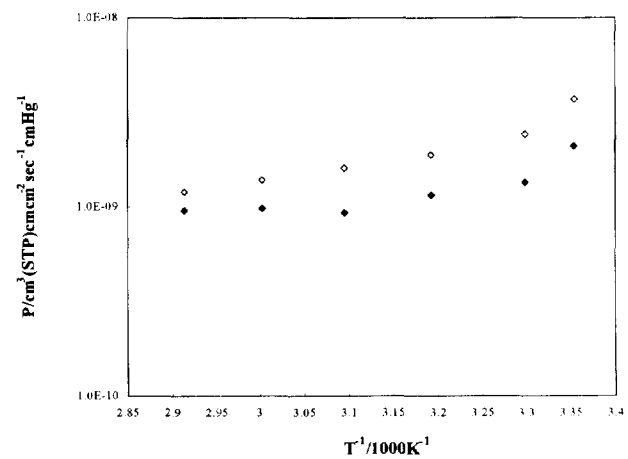


Figure 10 Comparison of permeability coefficients of 1-butene between PSMs doped with 2N AgBF₄ (♦) and AgNO₃ (◇) aqueous solutions as a function of reciprocal temperature

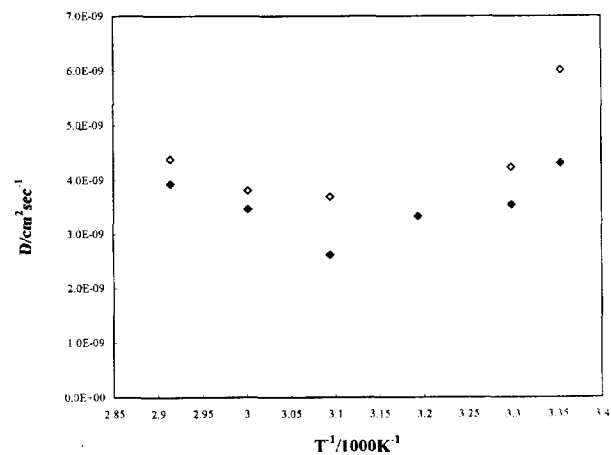


Figure 11 Comparison of apparent diffusion coefficients of 1-butene between PSMs doped with 2N AgBF₄ (♦) and AgNO₃ (◇) aqueous solutions as a function of reciprocal temperature

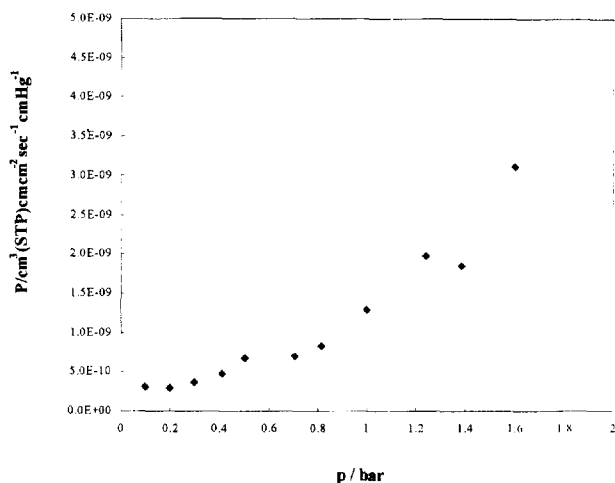


Figure 12 Permeability coefficients of 1-butene as a function of pressure of feed gas through PSM doped with 2N AgBF₄ aqueous solution

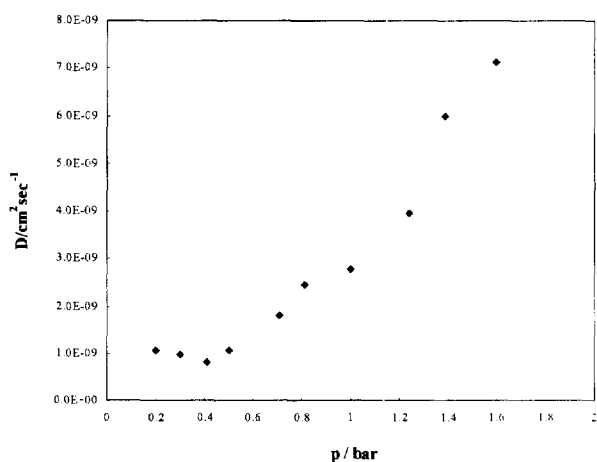


Figure 13 Apparent diffusion coefficients of 1-butene as a function of pressure of feed gas through PSM doped with 2N AgBF₄ aqueous solution at 25°C

which is suitable for permeation of *n*-butane through Ag⁺-doped PSM. This indicates that there must be a certain special transport mechanism based on the affinity between membrane and gas which controls the permeation of 1-butene through Ag⁺-doped PSM.

In order to discover the effect of the affinity between alkene and Ag⁺ on the permeation behaviour of 1-butene, the pressure dependence of *P* and *D* of 1-butene has been investigated and the results are shown in *Figure 12* and *Figure 13*, respectively. *Figure 14* and *Figure 15* also give out some typical curves of the relationship between transport parameters (*P* and *D*) and feed pressure *p* according to models suggested by other researchers for explicating various kinds of gas permeation behaviours previously^{28,29}. Obviously the transport of 1-butene through Ag⁺-doped PSM does not follow the dual-transport model usually being used to explain the gas permeation behaviour in glassy polymers either. In fact, our experiment data can be demonstrated well by the swelling model in glassy polymers although the permeability coefficient *P* does not increase with the decrease of *p* in the low pressure range. Being a kind of gas with high condense ability and owing to its special affinity with Ag⁺ inside the membrane, 1-butene may cause a rather strong swelling effect on the membrane.

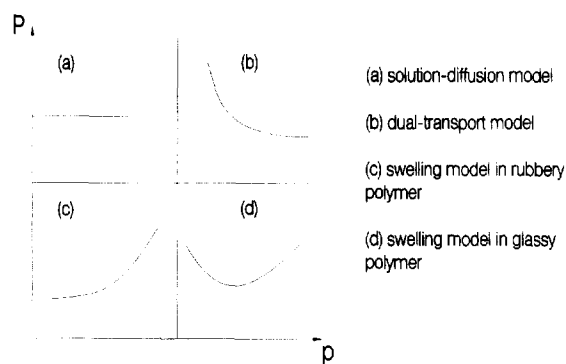


Figure 14 Typical Forms for pressure dependent permeability coefficients in polymeric media: (a) solution-diffusion model; (b) dual-transport model; (c) swelling model in rubbery polymer; (d) swelling model in glassy polymer

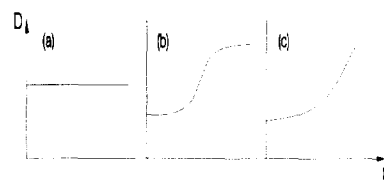


Figure 15 Typical forms for pressure-dependent apparent diffusion coefficient in polymeric media: (a) solution-diffusion model; (b) dual-transport model; (c) swelling model in rubbery polymer

So the swelling model, which we suggest here for the transport of 1-butene through Ag⁺-doped PSM membranes, can be described as following.

When 1-butene molecules reach the surface of the membrane, some of them are bound to the fixed Ag⁺ sites and the others are absorbed obeying the dual-sorption law. The molecules which are bound to Ag⁺ sites are fixed there and swell the polymer chains at the membrane surface. Other molecules diffuse into the membrane and propel this swelling effect along the direction of membrane thickness until the whole membrane is swollen.

Based on this swelling model, even though the fraction of 1-butene molecules adsorbed in the microvoids will increase as the pressure decreases in the low pressure range and then the solubility of the membrane is increased, the loss of diffusivity owing to the smaller degree of swelling of the membrane may play a more important role. So the pressure dependence curve of *P* exhibits the pattern of *Figure 12* without rolling up in the low pressure range.

Now consider the temperature dependence of permeability coefficient *P* and diffusion coefficient *D* again. At low temperature range, the binding of 1-butene to fixed Ag⁺ sites is fairly stable and the membrane is well swollen. This makes the diffusion of 1-butene molecules through the membrane rather easier so that high diffusivity and permeability can be obtained. As the temperature increases, the adsorption of 1-butene to Ag⁺ sites becomes more and more unstable. In this case the decrease of 1-butene concentration in the membrane will cause a drop of swelling degree and the diffusion coefficient *D*. On the other hand, the increase of temperature will enhance the mobility of polymer chains and let the transport of 1-butene through the membrane easier. As a result of the cooperation of these two factors, the diffusion coefficient *D* of 1-butene in Ag⁺-doped PSM membranes decreases with temperature (below 50°C) at first and then begins to increase as temperature

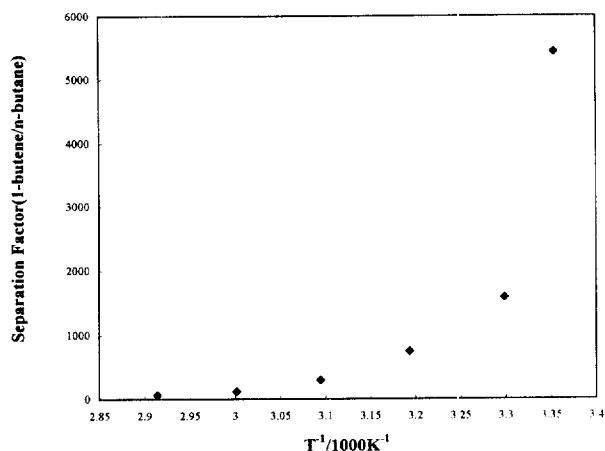


Figure 16 Ideal separation factor of 1-butene/n-butane with PSM doped in 2N $AgNO_3$ aqueous solution as a function of reciprocal temperature

arises. However, due to the solubility dependence on temperature, the permeability coefficient P keeps on decreasing even at high temperatures.

In *Figure 10* and *Figure 11* the permeability coefficients and the diffusion coefficients of 1-butene through PSM exchanged by $AgBF_4$ aqueous solution are compared with those through PSM exchanged by $AgNO_3$ aqueous solution. The curves have almost the same pattern. The only difference is that both the values of P and D in PSM exchanged by $AgBF_4$ solution is smaller than that in PSM exchanged by $AgNO_3$ solution. This phenomena can also be explained by the swelling model suggested in this paper. Since F atoms in $AgBF_4$ have stronger oxidation ability than O atoms in $AgNO_3$, they may weaken back-donation of d-electrons from occupied 4d orbitals of the silver ion into the unoccupied $\pi^* - 2p$ antibonding orbitals of the olefinic system. Therefore the affinity between Ag^+ and 1-butene is also weakened and then the alkene solubility in the membrane decreases. Thus, the membrane is less swollen and exhibits lower diffusivity and permeability.

Selectivity of 1-butene/n-butane

The ideal separation factor of 1-butene/n-butane in anhydrous Ag^+ -doped PSM as shown in *Figure 16*. The separation factor increases as temperature decreases until reaching 5443 at 25°C. This is a very high value compared with 100–200 which was obtained by W. S. Ho in his research on hydrated Ag^+ -PVA membranes³⁰. However, the P value of 1-butene in our anhydrous Ag^+ -doped PSM ($=3.73 \times 10^{-9} \text{ cm}^3 \text{ (STP) cm/cm}^2 \cdot \text{sec} \cdot \text{cmHg}$) is only 1/36 of W. S. Ho's membrane ($=135 \times 10^{-9} \text{ cm}^3 \text{ (STP) cm/cm}^2 \cdot \text{sec} \cdot \text{cmHg}$). That is, anhydrous membranes possess superiority on selectivity while hydrated membranes own superiority on permeability for olefin/paraffin gas mixtures.

In membrane separation processes, we often face the discrepancy of getting both high permeability and selectivity at the same time. If the permeability is enhanced by increasing temperature or adding water content in hydrated membranes, selectivity usually falls down. However, such a trade-off relationship does not appear in our Ag^+ -doped PSM. At low temperatures, both the permeability and selectivity reach their high values (*Figure 10* and *Figure 16*). This consistence indicates special predominance of our anhydrous Ag^+ -doped PSM in olefin/paraffin separation processes according to its swelling transport mechanism for alkenes.

Permeation of 1,3-butadiene and selectivity of 1-butene/1,3-butadiene

Figure 17 and *Figure 18* show the temperature dependence of P and D individually for 1,3-butadiene in anhydrous Ag^+ -doped PSM. The permeability coefficients and diffusion coefficients of 1,3-butadiene as a function of feed side pressure are also shown in *Figure 19* and *Figure 20* respectively. The style of all the curves is almost the same as that of 1-butene indicating the transport of 1,3-butadiene through Ag^+ -doped PSM is also controlled by the same swelling mechanism as 1-butene.

According to the research work of H. W. Quinn^{31,32}, 1,3-butadiene forms $AgBF_4 \cdot (1,3\text{-butadiene})$ complexes with $AgBF_4$ while 1-butene forms $AgBF_4 \cdot 2(1\text{-butene})$ complexes. This means the amount of 1,3-butadiene molecules that can be absorbed in Ag^+ -doped PSM is much less than that of 1-butene molecules, which leads to a lower swelling degree of the membrane. Furthermore, the rigidity of 1,3-butadiene is higher than 1-butene because it possesses two π -bonds in one molecule. It will certainly be more difficult for the more rigid molecule travelling in a membrane with the lower swelling degree. Comparing the values of P and D for 1,3-butadiene and 1-butene, agreement has been shown

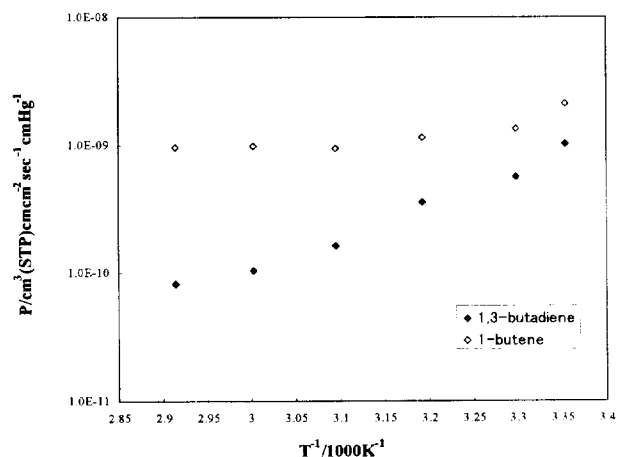


Figure 17 Permeability coefficients of 1,3-butadiene as a function of reciprocal temperature through PSM doped in 2N $AgBF_4$ aqueous solution compared with that of 1-butene

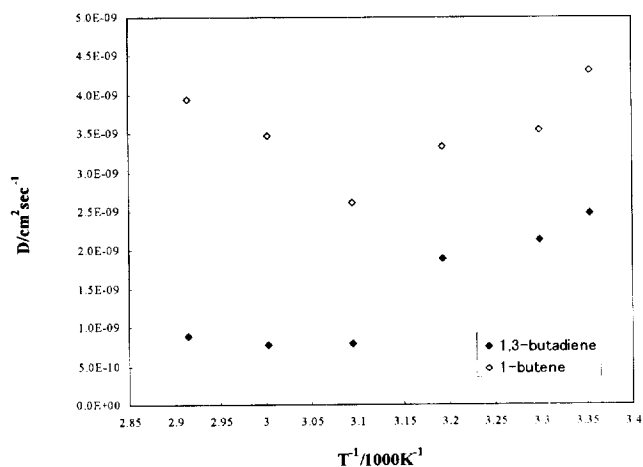


Figure 18 Apparent diffusion coefficients of 1,3-butadiene as a function of reciprocal temperature through PSM doped with 2N $AgNO_3$ aqueous solution, compared with that of 1-butene

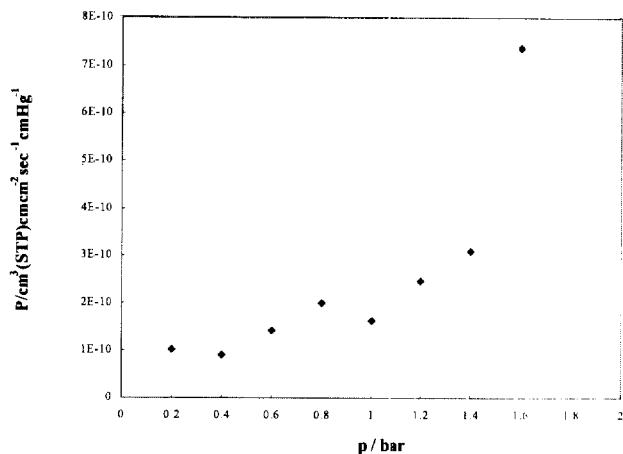


Figure 19 Permeability coefficients of 1,3-butadiene as a function of pressure of feed gas through PSM doped with 2N AgBF₄ aqueous solution

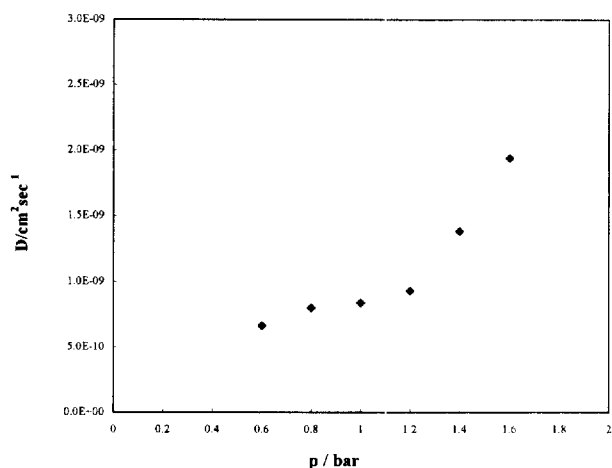


Figure 20 Apparent diffusion coefficients of 1,3-butadiene as a function of pressure of feed gas through PSM doped with 2N AgBF₄ aqueous solution at 25°C

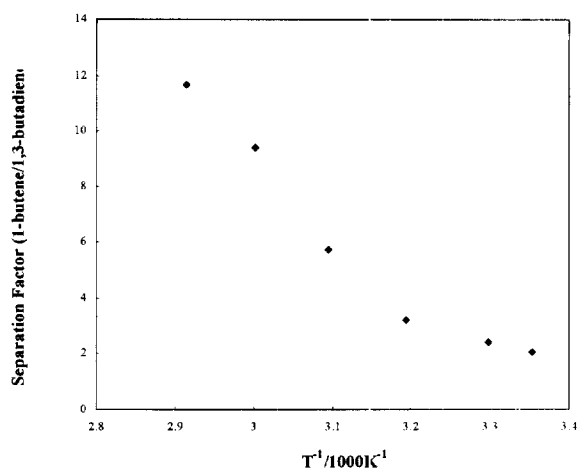


Figure 21 Ideal separation factor of 1-butene/1,3-butadiene with PSM doped in 2N AgBF₄ aqueous solution, as a function of reciprocal temperature

with the above discussion, that is, 1,3-butadiene exhibits lower diffusivity and permeability than 1-butene.

Figure 21 also gives out the variation of ideal separation factors of 1-butene/1,3-butadiene with temperature. A

trade-off relationship exists here, high selectivity appears at high temperatures while permeability prefers low temperatures. At 70°C (where $T^{-1} = 2.92 \times 10^{-3}$), the ideal separation factor is as high as 11.7 and the permeability coefficient of 1-butene is about 9.53×10^{-10} cm³ (STP)·cm/cm²·sec·cmHg, which is still a rather high value compared with other anhydrated membranes.

CONCLUSIONS

In order to understand the transport mechanism of olefin and paraffin through anhydrated Ag⁺-doped PSM, first characterization of the membrane was made by using EDS, positron annihilation lifetime measurement and AFM. The distribution of doped Ag⁺ in the membrane is homogeneous, no aggregation of silver ions on the surface is observed. Anhydrated Ag⁺-doped PSM are rather dense membranes and can dope Ag⁺ about two times as the concentration of charged group SO₃⁻ inside the membrane.

Then the permeation experiments were carried out for *n*-butane, 1-butene and 1,3-butadiene. Anhydrated Ag⁺-doped PSM exhibit high selectivity for the permeation of olefins. The ideal separation factor of 1-butene/*n*-butane is as high as 5443 in membranes exchanged by AgNO₃ aqueous solution. Both the permeability of 1-butene and selectivity of 1-butene/*n*-butane increase with the drop of temperature showing special predominance of the anhydrated Ag⁺-doped PSM used in this study. On the other hand, for 1-butene/1,3-butadiene system, the ideal separation factor increases with the temperature increase and reaches the value of 11.7 at 70°C while the permeabilities of these two olefins decrease with the temperature increase. The permeation of alkenes through anhydrated Ag⁺-doped PSM follows a swelling model which is suggested in this paper while the permeation behaviour of alkylene through anhydrated Ag⁺-doped PSM is controlled by simple solution-diffusion model. Based on such swelling mechanism, the diffusivity and permeability of alkenes are strongly affected by the amount of alkenes absorbed in the membrane. So the membranes with over-dope of Ag⁻ inside are rather prosperous ones for the separation of olefin/paraffin.

ACKNOWLEDGEMENTS

We are most grateful to Mr Hamada and Mr Yoshie of Asahi Chemicals Co Ltd, for providing us with the samples and for helpful suggestions.

REFERENCES

1. Eisenberg, A. and Yeager, H. L., *American Chemical Society*, Washington, DC, 1982.
2. Gronowski, A. A. and Yeager, H. L., *J. Electrochem. Soc.*, 1991, **138**, 2690.
3. Srinivasan, S., *J. Electrochem. Soc.*, 1989, **136**, 41c.
4. Poltarzewski, Z., Staiti, P., Alderucci, W., Wiczorek, W. and Giordano, N., *J. Electrochem. Soc.*, 1992, **139**, 761.
5. Parthasarathy, A., Dave, B., Srinivasan, S., Appleby, J. A. and Martin, C. R., *J. Electrochem. Soc.*, 1992, **139**, 1634.
6. Nagy, G., Gerhardt, G. A., Oke, A. F., Rice, M. E. and Adams, R. N., *J. Electroanal. Chem. Interfacial Electrochem.*, 1985, **188**, 85.
7. Malinski, T. and Taha, Z., *Nature*, 1992, **358**, 676.
8. Davis, J. C., Valus, R. J., Eshraghi, R. and Velikoff, A. E., *Sep. Sci. Technol.*, 1993, **28**, 463.
9. M. A. Kraus, *US Pat.* 4,614,524, 1986.
10. Koval, C. A. and Spontarelli, T., *J. Am. Chem. Soc.*, 1988, **110**, 293.
11. Koval, C. A. and Spontarelli, T., *Polym. Mater. Sci. Eng.*, 1988, **59**, 132.

12. Koval, C. A., Spontarelli, T. and Noble, R. D., *Ind. Eng. Chem. Res.*, 1989, **28**, 1020.
13. Koval, C. A., Spontarelli, T., Thoen, P. and Noble, R. D., *Ind. Eng. Chem. Res.*, 1992, **31**, 1116.
14. Beverwijk, C. D. M., Vander Kerk, G. J. M., Leusink, A. J. and Noltes, J. G., *Organometal. Chem. Rev. A*, 1970, **5**, 215.
15. Guo, B. C. and Castlemann, A. W., *Chem. Phys. Lett.*, 1991, **181**, 16.
16. Thoen, P. M., Noble, R. D. and Koval, C. A., *J. Phys. Chem.*, 1994, **98**, 1262.
17. Eriksen, O. I., Aksnes, E. and Dahl, I. M., *J. Membrane. Sci.*, 1993, **85**, 89.
18. Ho, W. S. and Dalrymple, D. C., *J. Membrane. Sci.*, 1994, **91**, 13.
19. Richter, C. and Woermann, D., *J. Membrane. Sci.*, 1994, **91**, 217.
20. Gierke, T. D., *J. Electrochem. Soc.*, 1977, **24**, 319c.
21. Gierke, T. D., Munn, G. E. and Wilson, F. C., *J. Polymer. Sci. Polym. Phys. Edn.*, 1981, **19**, 1687.
22. Hsu, W. Y. and Gierke, T. D., *J. Membrane. Sci.*, 1983, **13**, 307.
23. Noble, R. D., *J. Membrane. Sci.*, 1990, **50**, 207.
24. Rabago, R., Rryant, D. L., Koval, C. A. and Noble, R. D., *Ind. Eng. Chem. Res.*, 1996, **35**, 1090–1096.
25. Yamaguchi, T., Baertsch, C., Koval, C. A. and Noble, R. D., *J. Membrane. Sci.*, 1996, **117**, 151–161.
26. Mizoguchi, K., Hayamizu, K., Terada, K., Naito, Y. and Kamiya, Y., *Polym. Preprints Jpn.*, 1996, **45**, 2972.
27. Adachi, K., Matsumoto, H., Kawaguchi, S. and Tanioka, A., *Polym. Preprints. Jpn.*, 1996, **45**, 2972.
28. Yoshikazu, M., Ezaki, T., Sanui, K. and Ogata, N., *Koubunshi Ronbun.*, 1986, **43**, 729.
29. Koros, W. J. and Hellums, M. W., *Fluid Phase Equilibra*, 1989, **53**, 339.
30. Ho, W. S. and Dalrymple, D. C., *J. Membrane. Sci.*, 1994, **91**, 13.
31. Quinn, H. W. and Glew, D. N., *Can. J. Chem.*, 1962, **40**, 1103.
32. Quinn, H. W., *Can. J. Chem.*, 1967, **45**, 1329.